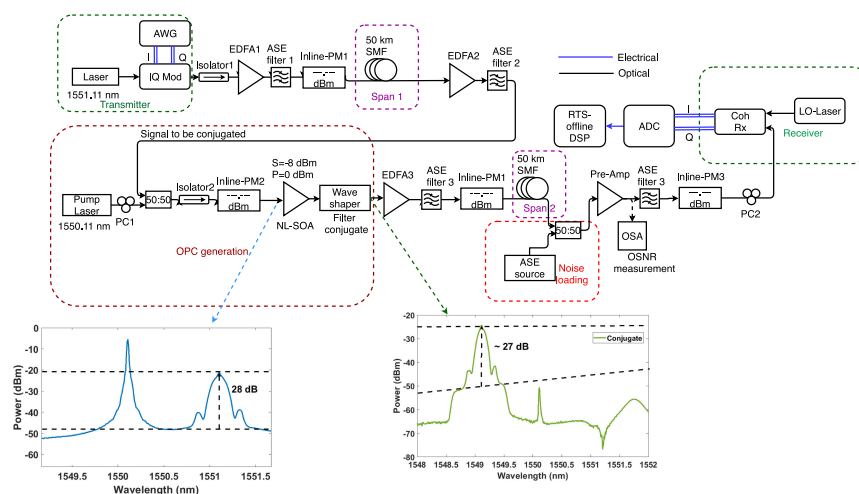


# Dispersion and Nonlinearity Distortion Compensation of the QPSK/16QAM Signals Using Optical Phase Conjugation in Nonlinear SOAs

Volume 12, Number 1, February 2020

Aneesh Sobhanan  
Lakshmi Narayanan Venkatasubramani  
R. David Koilpillai, *Member, IEEE*  
Deepa Venkitesh, *Member, IEEE*



DOI: 10.1109/JPHOT.2020.2964414

# Dispersion and Nonlinearity Distortion Compensation of the QPSK/16QAM Signals Using Optical Phase Conjugation in Nonlinear SOAs

Aneesh Sobhanan , Lakshmi Narayanan Venkatasubramani ,  
R. David Koilpillai, *Member, IEEE*,  
and Deepa Venkitesh , *Member, IEEE*

Department of Electrical Engineering, Indian Institute of Technology, Madras 600036, India

DOI:10.1109/JPHOT.2020.2964414

This work is licensed under a Creative Commons Attribution 4.0 License. For more information, see <https://creativecommons.org/licenses/by/4.0/>

Manuscript received November 17, 2019; revised December 18, 2019; accepted January 2, 2020. Date of publication January 6, 2020; date of current version January 24, 2020. This work was supported in part by the Office of the Principal Scientific Adviser, Govt. of India, in part by the Department of Science and Technology, Govt. of India, in part by the Ministry of Electronics and Information Technology, Govt. of India, and in part by the Visvesvaraya PhD scheme, Govt. of India. Corresponding author: Deepa Venkitesh (e-mail: [deepa@ee.iitm.ac.in](mailto:deepa@ee.iitm.ac.in)).

**Abstract:** We experimentally demonstrate the simultaneous compensation of both dispersion and nonlinear effects in a 100 km optical fiber link using optical phase conjugation of a 21 GB aud QPSK and 16QAM signal with nonlinear SOAs. Error-free performance is recorded for a launched power of up to 12 dBm, without any digital signal processing to compensate for distortions due to chromatic dispersion and nonlinear effects in fiber. The performance is verified for operation across the C-band.

**Index Terms:** Optical phase conjugation, semiconductor optical amplifier.

## 1. Introduction

Implementation of advanced modulation formats such as PM-QPSK and PM-16QAM has been possible in optical communication systems through efficient digital signal processing, typically at the receivers. The most commonly compensated impairments in such optical coherent communication links include phase noise of the transmitter and receiver lasers, frequency offset between the lasers, polarisation de-multiplexing, chromatic dispersion and clock recovery. In case of long fiber links, the overhead in digital signal processing (DSP) is the highest for chromatic dispersion compensation [1]. Nonlinear impairments in the fiber are typically avoided by controlling the optical power launched into the fiber. Even though advanced machine learning algorithms have been used in the recent past for nonlinearity compensation [2], the corresponding signal processing overheads are typically large. In this context, all-optical techniques - especially Optical Phase Conjugation (OPC) - with mid-span spectral inversion has proved to be effective in compensating for impairments induced by both dispersion and nonlinearity in fibers [3]–[7]. In addition, phase conjugation finds applications in time reversing the scattering processes for countering atmospheric turbulence and biological imaging in highly turbid samples [8]. Most of these demonstrations have used highly nonlinear fibers or periodically poled Lithium Niobate as the nonlinear medium - both of which require power levels, typically larger than 100 mW to initiate nonlinear effects. Nonlinear

semiconductor optical amplifiers (NL-SOAs)-on the other hand are compact and chip-integrable, where efficient nonlinear effects are observed even for pump power levels of  $\approx 0$  dBm. These have been used in the past to demonstrate various optical signal processing functionalities such as wavelength conversion [9]. Demonstration of optical phase conjugation with SOAs are however limited to intensity modulated signals [10], [11]. The most commonly quoted deterrents for these applications are the nonlinear chirp and the noise figure introduced by the SOA. However, we recently presented an experimental demonstration of OSNR retention of conjugate and signal along with chirp-free amplification of the signal with QPSK modulation in the presence of saturating pump [12]. These results indicate that the nonlinear chirp introduced by the SOA may not offer a significant penalty in conjugate generation.

In this work we experimentally demonstrate the mid-span spectral inversion (MSSI)-aided nonlinearity and CD compensation of a 21 Gbaud QPSK and 16QAM signal, using a nonlinear SOA in a two-span link, with each span of length 50 km. The residual penalty due to the nonlinear chirp introduced by SOA is evaluated by measuring the BER as a function of optical signal to noise ratio (OSNR) at the receiver. The nonlinearity compensation is demonstrated by evaluating the performance of the link for different power levels launched in to the fiber. We believe this is the first demonstration of simultaneous dispersion and nonlinearity compensation using a nonlinear SOA for QPSK and 16QAM signals.

## 2. Theory

The mathematical analysis of OPC based Kerr nonlinearity and dispersion compensation is well established in literature [13]. The signal transmission through a nonlinear ( $\gamma$ ), dispersive ( $\beta_2$ ) and lossy ( $\alpha$ ) medium is described by nonlinear Schrodinger equation (NLSE) given as,

$$\frac{\partial A(z, t)}{\partial z} + \frac{i}{2}\beta_2 \frac{\partial^2 A(z, t)}{\partial t^2} - i\gamma |A(z, t)|^2 A(z, t) + \frac{\alpha}{2} A(z, t) = 0. \quad (1)$$

Equation (1) shows the evolution of the complex envelope of the signal ( $A$ ) through the first span of the fiber. Conjugate of the signal ( $A^*$ ) is generated through OPC. The NLSE for the propagation of conjugate through the second span of the fiber can be written as,

$$\frac{\partial A^*(z, t)}{\partial z} - \frac{i}{2}\beta_2 \frac{\partial^2 A^*(z, t)}{\partial t^2} + i\gamma |A^*(z, t)|^2 A^*(z, t) + \frac{\alpha}{2} A^*(z, t) = 0. \quad (2)$$

Note that the signs of the second and third terms in Eqn (1) are inverted for the propagation of conjugate. Thus, the dispersive and nonlinear phase accumulated in the first span can be compensated when the conjugate is transmitted through an equal length of the second span of fiber with identical  $\beta_2$  and  $\gamma$ , assuming identical launched powers [13]. The optical phase conjugate is generated using partially degenerate four wave mixing in SOA. Considering a signal at frequency  $\omega_s$  with line width  $\Delta\nu_s$ , and pump at frequency  $\omega_p$  with line width  $\Delta\nu_p$  are the input to the SOA, the conjugate at  $2\omega_p - \omega_s$  is generated in the SOA with a line width of  $4\Delta\nu_p + \Delta\nu_s$  [14]. In addition, the SOA is expected to introduce nonlinear phase distortions depending on the bias current and the input power levels. Thus the optical phase conjugate generated in SOA is expected to have a penalty with respect to the back-to-back back signal performance due to the inherent phase distortion in SOA and the phase noise transfer during the OPC generation process. However, considering the compact size and the relatively smaller power levels required for conjugate generation, we proceed to demonstrate dispersion and non-linearity compensation with an SOA.

## 3. Experimental Setup

The schematic of the experimental set up to demonstrate dispersion and nonlinearity compensation with mid-span spectral inversion using SOA is shown in Fig. 1. A narrow-line laser of wavelength 1551.11 nm is modulated with 21 Gbaud QPSK using an IQ modulator driven by an arbitrary wave generator (AWG, 64 GSa/s). The modulated signal is fed to the first span of standard single mode fiber (G.652D) of length 50 km through an erbium doped fiber amplifier (EDFA1) and an in-line

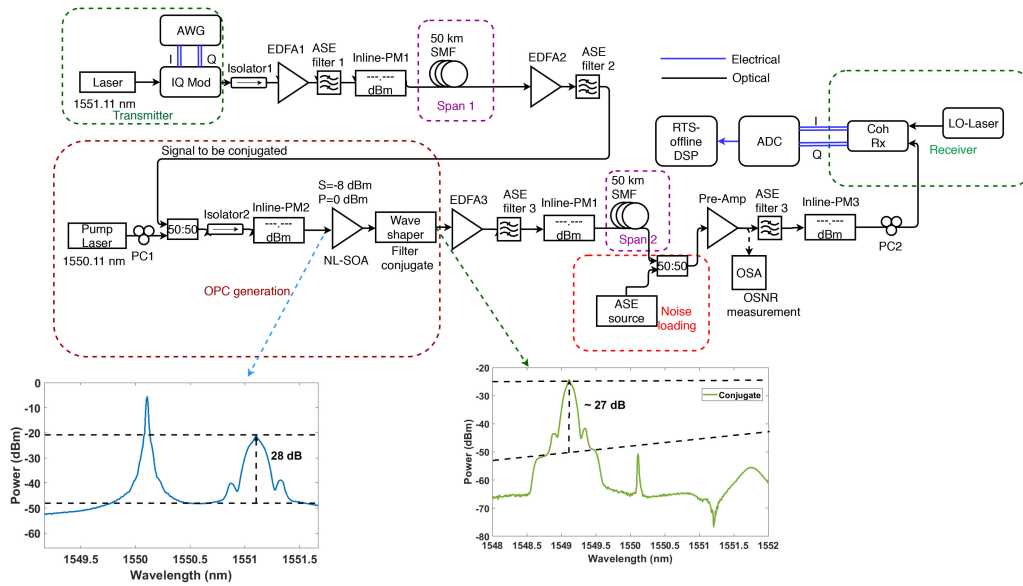


Fig. 1. Schematic of the experimental setup to demonstrate dispersion and nonlinearity compensation using mid-span spectral inversion with a nonlinear SOA. Spectra at the input and filtered conjugate output are shown as insets for reference.

power monitor (PM) such that the average power at the input of the first span is maintained at 0 dBm. The signal power launched into the OPC stage is maintained at  $-8$  dBm, by appropriately amplifying it through EDFA2. The pump laser at wavelength 1550.11 nm (corresponding to a pump-signal detuning of 125 GHz) with 0 dBm power is used to saturate the NL-SOA and initiate the four wave mixing processes in the SOA. The nonlinear SOA used in our experiments has an output saturation power of 11.5 dBm and a carrier recovery time of 25 ps. The phase conjugate is generated at 1549.11 nm due to the partially degenerate four-wave mixing (FWM) process. The spectra at the input, output of SOA and after filtering is shown as insets in Fig. 1 for reference. The phase conjugate is filtered, amplified using EDFA3 and is fed to second span of a similar G.652D fiber of length 50 km. The OSNR of the signal/conjugate is controlled by introducing ASE noise from an EDFA at the coherent receiver.

The received signal is further digitized using a real-time scope (80 GSa/s). The digitized output is post-processed using off-line DSP, and the specific algorithms used are discussed in later sections. For the C-band experiment, both the signal and the pump wavelength are swept over C-band while maintaining the detuning of 125 GHz between them.

#### 4. Results and Discussion

Figure 2(a) shows the BER performance as a function of OSNR for a different operating conditions. The “b2b signal,” (shown as points with open red circles) represents the performance of the modulated signal without including the fiber and OPC stage; these results are further used as reference to calculate the OSNR penalty. The sequence of DSP algorithms used for post processing are: frequency offset compensation using the periodogram technique, phase noise correction using the Decision-Directed Least Mean Squares (DD-LMS) algorithm [15], followed by clock recovery and demodulation [16]. The signal is now fed to the OPC stage and the BER performance of the conjugate is studied as a function of OSNR of the conjugate. These results are shown as blue open circles with the legend “b2b-OPC”. The off-line DSP algorithms used is the same as before, and the BER is estimated with respect to the conjugate data in this case.

Figure 2(a) shows a penalty of about 1 dB for “b2b-OPC” with respect to the back-to-back case because of (a) phase noise transfer from the pump laser, inherent to the degenerate mixing

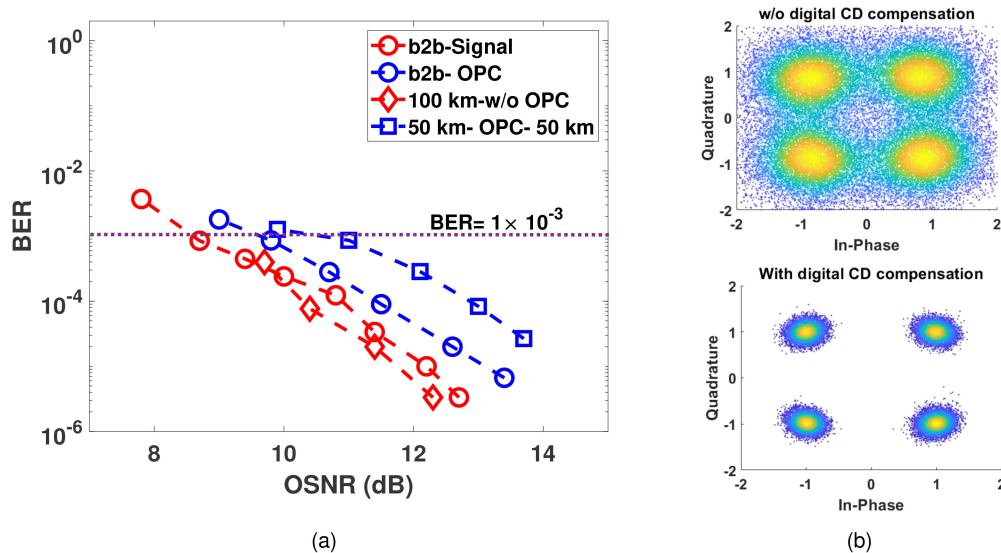


Fig. 2. (a) BER performance as a function of different OSNR values for 40 Gbps QPSK signal- b2b: back-to-back performance without the 100 km link. (b) 21 GBaud QPSK signal Constellation after 50 km for an OSNR of 27 dB for both without digital CD compensation (BER = 0.5, fails in proper demodulation), and with digital CD compensation (BER = 0).

process [17] and (b) due to the inherent nonlinear phase distortion in SOA. The performance of the system with 100 km fiber is now ascertained without OPC and are shown in open diamonds in red. In addition to phase noise compensation and frequency offset correction the off-line DSP in this case also includes dispersion compensation using frequency domain equalization [1]. These results are identical to that of the back-to-back case since the dispersion introduced by the fiber is fully compensated by DSP.

The total ISI in a 50 km link is about 6 symbols while it is about 12 symbols in a 100 km link. Note that, even in case of 50 km, the data cannot be demodulated without applying a dispersion compensation algorithm. Fig. 2(b) shows the constellation of 21 GBaud QPSK signal at the output of 50 km fiber for an OSNR of 27 dB for the case (a) without digital CD compensation (b) with digital CD compensation. It is evident that ISI corresponding to even 6 symbols leads to a significant distortion. Thus, SOA-based OPC indeed has a significant role to play even when the ISI is as small as 12 symbols (6 symbols from first fiber span and 6 symbols from next fiber span).

We now include the OPC stage in the mid-span, where the signal after one span is launched at the input of the nonlinear SOA, along with a CW pump of power 0 dBm, with a detuning of 1 nm with respect to the signal. A conjugate conversion efficiency of  $-3$  dB is obtained. The conjugate is further propagated through the second span, and it is expected that the phase accumulated in the signal due to chromatic dispersion will be compensated in the conjugate wavelength at the end of the second span. The off-line DSP in this case does not include dispersion compensation. BER performance is ascertained as a function of conjugate OSNR, and we find a penalty of less than 1.5 dB (at FEC limit BER) with respect to the “b2b-OPC” case. This additional penalty is potentially due to the nonlinear chirp accumulated in the SOA. An overall penalty of  $<2.5$  dB is observed with respect to the back-to-back case. This OSNR penalty can be potentially compensated by launching larger power into the system. However, this may increase the nonlinear penalties. We now proceed to evaluate the resilience of nonlinearities to the SOA-based OPC generation system.

The power launched into each span is now increased in steps of 2 dBm, and the performance of the system is evaluated for the case without OPC and with OPC. Care is taken to ensure that the launched power in each span is identical, while the signal power at the input of the OPC stage is maintained at  $-8$  dBm. The pump power is maintained at 0 dBm in all cases. The EVM is found

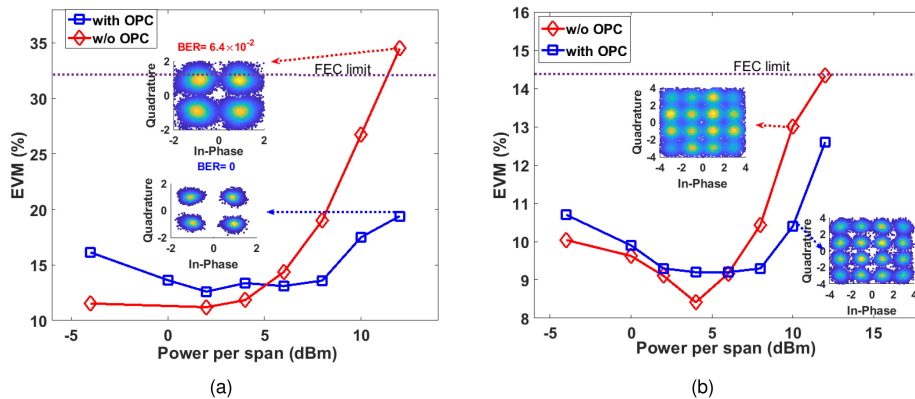


Fig. 3. EVM as a function of input launch power to each 50 km fiber span, in the presence and absence of OPC (a) 40 Gbps QPSK and (b) 80 Gbps 16 QAM.

out for both cases and shown as a function of power launched in each span. We carry out this experiment for both QPSK and 16QAM modulations with corresponding data rates of 40 Gbps and 80 Gbps and the results are shown in Fig. 3(a) (a) and 3(b) (b) respectively.

Drop in EVM with the increase in the power per span is due to a corresponding increase in the OSNR at the input. The drop is more evident in 16-QAM case (Fig. 3(b)) as the phase margin of the 16QAM format ( $16.9^\circ$ ) is much smaller compared to the QPSK format ( $45^\circ$ ) [18] and is more sensitive to even the smaller variation of OSNR. As the input power increases further, the nonlinear distortions would result in an increase in EVM, as indicated in Fig. 3(a) and 3(b). In the presence of OPC, the power at which the EVM starts to degrade is larger, indicating the nonlinear tolerance of the system.

As expected, for smaller values of input powers, the performance of the OPC system is poorer for both QPSK and 16QAM, which is primarily due to the phase noise transfer from the pump and the nonlinear chirp due to the SOA. The largest penalty in the smallest launch power ( $-4$  dBm) can be also attributed to the lower conversion efficiency and the lower output OSNR of the optical phase conjugate at lower input OSNR even though the input signal to SOA is maintained at  $-8$  dBm. For QPSK and QAM signals, however, the EVM is maintained constant (14% for QPSK and 9.5% for 16QAM within 0.5% change) up to 8 dBm launch power. The data is retrieved with 0 BER for QPSK and below FEC limit for 16QAM signals even at a launch power of 12 dBm when OPC is used in the link. For the system without OPC, the EVM penalty starts increasing significantly for input power levels of larger than 8 dBm due to nonlinear effects introduced in the fiber. The nonlinear effects accumulated by the signal in the first span is compensated by the conjugate propagation in the second span, thereby providing reduced penalties even at larger input power levels. To emphasize the results, QPSK constellations at 12 dBm launch power for both with and without OPC systems are shown in Fig. 3(a). The BER is increased to  $6.4 \times 10^{-2}$ , which is above FEC limit when system has no OPC, whereas the system gives error free performance when OPC is included. We thus prove that, even though the SOA-based OPC has an OSNR penalty of 2.5 dB, the same can be easily compensated using larger input power levels. We additionally observe that the link distances can be extended further since a power level of even up to 12 dBm can be launched into the fiber. Note that even an input power of 12 dBm per span has not resulted in an EVM corresponding to the FEC limit. Referring to Fig. 3(a) and 3(b), considering an EVM of 20 % for QPSK (and 10 % for 16QAM), the power margin with OPC is found to be 4 dB (and 2 dB for 16QAM). This power margin between the cases with OPC and without OPC could be slightly higher if the total mid span length is higher (say 500 km each) as the nonlinear distortion increases with length. This can be further experimentally ratified in long-haul systems.

We now proceed to evaluate the performance of the SOA-based OPC across the C-band. Fig. 4, shows the EVM evaluated for both QPSK and 16 QAM signals in a 100 km link when the launch

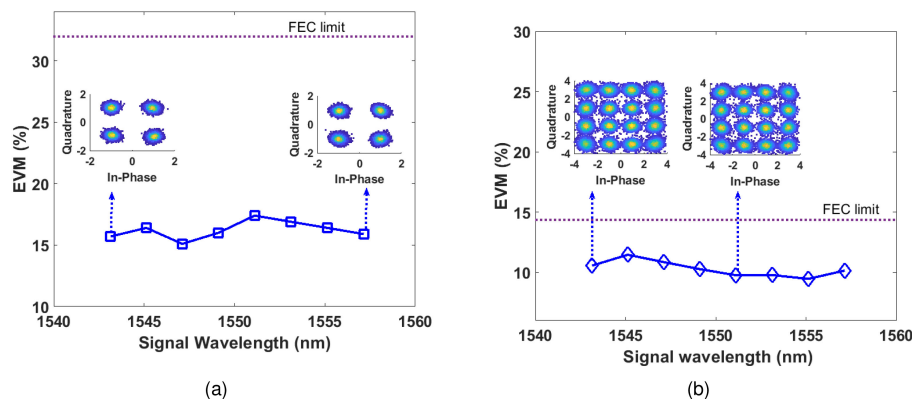


Fig. 4. EVM throughout the C-band when OPC is used in the link with a per span launch power of 10 dBm (a) 40 Gbps QPSK and (b) 80 Gbps 16QAM.

power per span is 10 dBm each throughout the C-band. For QPSK, the EVM is around 16% throughout the C-band and for 16 QAM it is 10% with a  $\pm 1\%$  variance. However, all the points in the Fig. 4(a) has an error free performance, and the points in the Fig. 4(b) has BER below FEC limit. Thus the OPC generation and its utility for impairment compensation using nonlinear SOA for entire C-band is experimentally demonstrated successfully.

## 5. Conclusion

We have experimentally demonstrated the feasibility of nonlinear SOA as a medium for optical phase conjugation process. Using OPC in NL-SOA a simultaneous compensation of nonlinearity and chromatic dispersion is achieved with a performance improvement which gives an error free performance up to 12 dBm launch power. The SOA-based OPC has a penalty of around 2.5 dB in a link operating in the linear regime. The phase noise transfer in OPC generation and the nonlinear phase distortion in SOA are the major performance degrading factors. An independent study has been carried out to reduce this phase distortion from the nonlinear SOAs during the conjugation process. However, by launching larger power, overall increase in reach can be obtained, and that too without any digital signal processing for dispersion and nonlinearity compensation. This scheme can be further extended to polarization multiplexed configuration based on the polarization insensitive implementation reported in [19]. We also demonstrate conjugate generation in the entire C-band with the SOA, and hence the results presented in this paper provides a pathway for all-optical dispersion compensation and nonlinearity compensation for a practical link, using compact and energy efficient nonlinear SOA. Even though the demonstration in this paper is limited to 100 km link we do not expect any change in penalty with the use of NL-SOA in a long-haul link, so long as SOA-OPC stage is placed in the mid-span. Compared to other optical signal processing media such as HNLf, PPLN, Silicon waveguide which consume several Watts of optical pump power for efficient conjugate generation, SOA requires only  $<1$  dBm pump power for a good conversion efficiency. The consequent reduction in the energy per bit for achieving the nonlinear operation and its compact implementation are compelling reasons to use SOAs as an attractive choice for optical signal processing applications.

## Acknowledgment

The authors would like to thank Sterlite Technologies for providing the fiber and K. Vijay and Anirudh.V for fruitful technical discussions.

---

## References

- [1] S. J. Savory, G. Gavioli, R. I. Killey, and P. Bayvel, "Electronic compensation of chromatic dispersion using a digital coherent receiver," *Opt. Express*, vol. 15, no. 5, pp. 2120–2126, Mar. 2007.
- [2] A. Amari, X. Lin, O. A. Dobre, R. Venkatesan, and A. Alvarado, "A machine learning-based detection technique for optical fiber nonlinearity mitigation," *IEEE Photon. Technol. Lett.*, vol. 31, no. 8, pp. 627–630, Apr. 2019.
- [3] T. Umeki *et al.*, "Simultaneous nonlinearity mitigation in  $92 \times 180$ -Gbit/s PDM-16QAM transmission over 3840 km using PPLN-based guard-band-less optical phase conjugation," *Opt. Express*, vol. 24, no. 15, pp. 16945–16951, Jul. 2016.
- [4] M. A. Z. Al-Khateeb *et al.*, "Experimental demonstration of 72% reach enhancement of 3.6Tbps optical transmission system using mid-link optical phase conjugation," *Opt. Express*, vol. 26, no. 18, pp. 23960–23968, Sep. 2018.
- [5] M. Al-Khateeb, M. Tan, T. Zhang, and A. D. Ellis, "Combating fiber nonlinearity using dual-order raman amplification and OPC," *IEEE Photon. Technol. Lett.*, vol. 31, no. 11, pp. 877–880, Jun. 2019.
- [6] K. R. H. Bottrill, N. Taengnoi, F. Parmigiani, D. J. Richardson, and P. Petropoulos, "PAM4 transmission over 360 km of fibre using optical phase conjugation," *OSA Continuum*, vol. 2, no. 3, pp. 973–982, 2019.
- [7] M. A. Z. Al-Khateeb, M. E. McCarthy, C. Sanchez, and A. D. Ellis, "Nonlinearity compensation using optical phase conjugation deployed in discretely amplified transmission systems," *Opt. Express*, vol. 26, no. 18, pp. 23945–23959, Sep. 2018.
- [8] A. Mosk, A. Lagendijk, G. Lerosey, and M. Fink, "Controlling waves in space and time for imaging and focusing in complex media," *Nature Photon.* vol. 6, pp. 283–292, 2012.
- [9] A. P. Anthur, R. T. Watts, K. Shi, J. O' Carroll, D. Venkitesh, and L. P. Barry, "Dual correlated pumping scheme for phase noise preservation in all-optical wavelength conversion," *Opt. Express*, vol. 21, no. 13, pp. 15568–15579, Jul. 2013.
- [10] M. C. Tatham, G. Sherlock, and L. D. Westbrook, "Compensation fibre chromatic dispersion by optical phase conjugation in a semiconductor laser amplifier," *Electron. Lett.*, vol. 29, no. 21, pp. 1851–1852, Oct. 1993.
- [11] W. Pieper *et al.*, "Nonlinearity-insensitive standard-fibre transmission based on optical-phase conjugation in a semiconductor-laser amplifier," *Electron. Lett.*, vol. 30, no. 9, pp. 724–726, Apr. 1994.
- [12] A. Sobhanan, V. A. M. Karthik, L. V. Narayanan, R. D. Koilpillai, and D. Venkitesh, "Experimental analysis of noise transfer in optical phase conjugation process in nonlinear SOA," in *Proc. Opt. Fiber Commun. Conf. Exhib.*, 2019, pp. 1–3.
- [13] C. Lorattanasane and K. Kikuchi, "Design theory of long-distance optical transmission systems using midway optical phase conjugation," *J. Lightw. Technol.*, vol. 15, no. 6, pp. 948–955, Jun. 1997.
- [14] R. Hui and A. Mecozzi, "Phase noise of fourwave mixing in semiconductor lasers," *Appl. Phys. Lett.*, vol. 60, no. 20, pp. 2454–2456, 1992.
- [15] I. Fatadin, D. Ives, and S. J. Savory, "Blind equalization and carrier phase recovery in a 16-QAM optical coherent system," *J. Lightw. Technol.* vol. 27, no. 15, pp. 3042–3049, Aug. 2009.
- [16] S. J. Varughese, V. Mathew, S. Swain, D. Venkitesh, and R. D. Koilpillai, "200G system with PDM-16QAM: Performance evaluation and trade-offs," in *Proc. 21st Nat. Conf. Commun.*, 2015, pp. 1–6.
- [17] J. Zhou, R. Hui, and N. Caponio, "Spectral linewidth and frequency chirp of four-wave mixing components in optical fibers," *IEEE Photon. Technol. Lett.*, vol. 6, no. 3, pp. 434–436, Mar. 1994.
- [18] M. Paskov, "Algorithms and Subsystems for Next Generation Optical Networks," 2015.
- [19] A. Sobhanan, L. N. Venkatasubramani, R. D. Koilpillai, and D. Venkitesh, "Polarization-insensitive phase conjugation of QPSK signal using Bragg-scattering FWM in SOA," *IEEE Photon. Technol. Lett.*, vol. 31, no. 12, pp. 919–922, Jun. 2019.